J Biomol NMR (2007) 38:65–72
DOI 10.1007/s10858-007-9147-9

ARTICLE

Measurement of dissociation constants of high-molecular weight protein–protein complexes by transferred ^{15}N-relaxation

Xun-Cheng Su · Slobodan Jergic · Kiyoshi Ozawa · Nicolas Dale Burns · Nicholas E. Dixon · Gottfried Otting

Received: 19 November 2006 / Accepted: 16 January 2007 / Published online: 28 March 2007

Abstract The use of ^{15}N-relaxation data for determination of the dissociation constant of a protein–protein complex is proposed for the situation where a ^{15}N-labeled protein is bound to an unlabeled protein of high molecular weight, and the chemical exchange between bound and free protein is fast on the NMR time scale. The approach is shown to be suitable for estimating dissociation constants in the micromolar to millimolar range, using protein solutions at relatively low concentration. An example is shown for the interaction between two subunits from the *Escherichia coli* DNA polymerase III complex, involving a ^{15}N-labeled fragment of the C-terminal domain of the τ subunit (15 kDa) and the unlabeled α subunit (130 kDa).

Keywords ^{15}N relaxation · Chemical exchange · Dissociation constant · *E. coli* DNA polymerase III · Protein–protein complex · Subunits α and τ

Introduction

NMR spectroscopy is widely used for the characterization of protein–protein and protein–ligand interactions (Dwek 1975; Otting 1993; Walters et al. 1999; Howard et al. 2000; Zuiderweg 2002; Bonvin et al. 2005; Takeuchi and Wagner 2006; Vaynberg and Qin 2006). Compared to other biophysical techniques, NMR spectroscopy is particularly suitable for the measurement of dissociation constants in the high micromolar and low millimolar range. In the limit of fast chemical exchange, dissociation constants are readily measured by monitoring NMR parameters as a function of ligand concentration (Garrett et al. 1997). Most frequently, chemical shift changes are monitored. Yet, this approach becomes difficult in the case of two weakly binding proteins where the accessible concentration ranges are limited, so that the limiting chemical shift value in the bound state cannot be established.

A growing number of recent experimental studies has focused on interactions between proteins and binding partners of molecular weights > 100 kDa, using peak height analysis (Matsuo et al. 1999; Howard et al. 2000), transferred cross saturation (Nakanishi et al. 2002), and ^{1}H relaxation measurements (Sui et al. 2005). These studies were directed at obtaining structural information about the protein interface rather than binding-affinities, and often depended on the availability of perdeuterated samples.

Here we analyze the potential of using transferred ^{15}N-relaxation for estimating the binding affinity of a 10–20 kDa protein, labeled only with ^{15}N, to an unlabeled protein with a molecular weight > 100,000. In the limit of fast chemical exchange, the relaxation rates in the bound and the free state are averaged so that the fraction of bound protein can be obtained by comparison of the ^{15}N-relaxation rates in the free protein with the rates expected in the protein–protein complex. In the case of high-molecular weight binding partners, where the average $R_2(^{15}\mathrm{N})$ relaxation is dominated by the relaxation in the bound state, the measurements can be referred to as transferred ^{15}N-relaxation experiments, in analogy to transferred NOE (Clore and Gronenborn 1982, 1983), transferred cross-correlation (Carlomagno et al. 1999), and transferred pseudocontact shift (John et al. 2006) experiments. Although estimates of the relaxation times in the complex

X.-C. Su · S. Jergic · K. Ozawa · N. D. Burns · N. E. Dixon · G. Otting (✉)
Research School of Chemistry, Australian National University, Canberra ACT 0200, Australia
e-mail: Gottfried.Otting@anu.edu.au

may be inaccurate, any other parameter accessible to NMR measurements of low-molecular weight systems would, in most cases, be even harder to estimate for the high-molecular weight complex. Since the sensitivity of modern NMR spectrometers permits ^{15}N-relaxation measurements of 100 μM protein solutions and many large protein complexes are soluble at this concentration, the use of ^{15}N-relaxation data for the measurement of dissociation constants has become a genuine option, motivating a more detailed analysis.

Experimental data are presented for the interaction between the α subunit and the C-terminal Domain V of the τ subunit of the *Escherichia coli* DNA polymerase III. The α subunit has a molecular weight of ~130,000, and the Domain V of the τ subunit (τ_C16, residues 499–643) has a molecular weight of ~16,000. While τ_C16 binds to α with picomolar affinity (Gao and McHenry 2001; Jergic et al. 2007), a construct shortened by 11 residues at the C-terminus (τ_C16Δ11; 15 kDa) binds more weakly with rapid chemical exchange between bound and free τ_C16Δ11. ^{15}N-relaxation measurements were made with a ^{15}N-labeled sample of τ_C16Δ11 in the absence and presence of unlabeled α to estimate the contribution of the τ_C16Δ11 fragment to the overall binding affinity of τ to α.

Methods

The proteins τ_C16Δ11 and α were overproduced and purified as described elsewhere (Wijffels et al. 2004; Jergic et al. 2007). All samples for NMR measurements were prepared in a buffer containing 10 mM phosphate (pH 6.8), 100 mM NaCl, 1 mM dithiothreitol, and 0.1 mM NaN_3 in 90% H_2O/10% D_2O. Solutions with different ratios of τ_C16Δ11 and α were prepared by titration of a 1.5 mM stock solution of ^{15}N-labeled τ_C16Δ11 into a 0.12 mM solution of α.

^{15}N-relaxation data were recorded at 25°C on a Bruker Avance 800 NMR spectrometer equipped with a TCI cryoprobe. ^{15}N-relaxation measurements used the experiments by Farrow et al. (1994), using protein concentrations of 350 μM τ_C16Δ11 for measurements in the absence of α, and 460 μM τ_C16Δ11 and 83 μM α for the complex. The relaxation delays were 9, 17, 26, 43, 60, 69, 86, and 104 ms in the R_2 experiment and 3, 70, 100, 300, 500, 750, 1000, and 1400 ms in the R_1 experiment. The relaxation delay of the R_2 experiment contained a CPMG train of 180°(^{15}N) pulses spaced by 900 μs. The complete set of R_1 and R_2 relaxation data was recorded in about 18 h, using t_{1max} = 50 ms and t_{2max} = 100 ms for each spectrum.

Mathematica (Wolfram Research, Champaign, USA) was used to simulate the curves in Fig. 2.

Results and discussion

Conditions for transferred relaxation

We assume a two-state equilibrium between a small ^{15}N-labeled protein A and a large unlabeled protein B,

$$A + B \underset{k_{off}}{\overset{k_{on}}{\rightleftharpoons}} AB \quad (1)$$

where k_{on} and k_{off} are the association and dissociation rate constants, respectively, and the dissociation constant $K_D = k_{off}/k_{on}$. The transferred relaxation experiment relies on fast chemical exchange, so that the relaxation rates are averaged between the bound and the free state (Fushman et al. 1997):

$$R_{1av} = (1 - p_B)R_{1free} + p_B R_{1bound} \quad (2)$$

$$R_{2av} = (1 - p_B)R_{2free} + p_B R_{2bound} \quad (3)$$

where p_B is the fraction of protein A engaged in the complex AB, R_{1av} and R_{2av} are the longitudinal and transverse relaxation rates measured for protein A in the presence of protein B, $R_{1free}$and R_{2free} are the corresponding relaxation rates measured in the absence of B, and R_{1bound} and R_{2bound} are the relaxation rates in the complex AB.

$R_2(^{15}N)$ relaxation rates of globular proteins are, in first approximation, directly proportional to the molecular weight (Fig. 1; Fushman et al. 2004; Ryakov et al. 2006). Therefore, p_B can be determined using a value of R_{2bound} estimated from the molecular weight of the complex, and R_{2free} and R_{2av} data measured experimentally. p_B is related to the dissociation constant K_D

$$K_D = [B_{tot}](1 - p_B)(1 - p_B[A_{tot}]/[B_{tot}])/p_B \quad (4)$$

where $[A_{tot}]$ and $[B_{tot}]$ denote the total concentrations of proteins A and B.

If protein B is much larger than protein A, the average $R_2(^{15}N)$ relaxation rate reflects the presence of even a small population p_B of protein A in the complex. In contrast, $R_1(^{15}N)$ relaxation decreases with increasing molecular weight, resulting in much smaller effects of protein B on the $R_1(^{15}N)$ relaxation rates of protein A. Therefore, in contrast to interaction studies of low-molecular weight compounds with proteins (Peng et al. 2004), R_1 relaxation measurements are not suitable for measurements of the binding affinity of two proteins.

Averaging of the $R_2(^{15}N)$ relaxation rates according to Eq. 3 requires (i) that the averaging of the NMR signals is sufficiently fast on the chemical shift time scale to prevent contributions to R_2 from chemical exchange and (ii) that the exchange rate between bound and free protein is faster

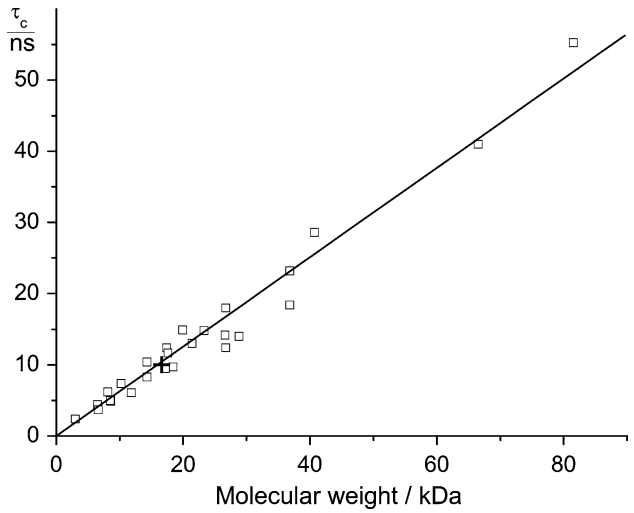

Fig. 1 Experimentally determined average rotational correlation times τ_C (as reported in Table 1 of Ryabov et al. (2006)) versus molecular weight (determined from the SEQRES entries of the respective PDB files). The τ_C values refer to aqueous solutions at 20°C. The cross marks the average rotational correlation time of the N- and C-terminal domains of calmodulin (Barbato et al., 1992), scaled from the temperature of the experiment (35°C) to 20°C using the equation reported in Table 1 of Ryabov et al. (2006)

than the R_2 relaxation rate in the bound state. The first condition is readily fulfilled for nuclei located far from the protein–protein interface for which the chemical shifts are the same in the free and the bound state. The second condition needs closer inspection. For example, for K_D = 10^{-4} M and a diffusion-controlled protein association rate k_{on} of 10^6 M^{-1} s^{-1}, k_{off} is 100 s^{-1}. This is of the same order of magnitude as the $R_2(^{15}N)$ relaxation rate expected for a 100 kDa protein complex.

It is instructive to explore this limiting regime by line shape analysis. The line shape expected for a 2-site exchange system with different populations in sites A and B can be calculated accurately for any exchange and intrinsic relaxation rates in the two sites (Swift and Connick 1962; Sandström 1982). We probed the validity range of Eq. 3 by simulating the line shapes and converting the resulting full line width at half height $\nu_{1/2}$ into an apparent R_2 relaxation rate of protein A, using $R_2 = \nu_{1/2}\pi$. Figure 2A shows representative examples of the apparent R_2 relaxation rate for 2-site exchange with R_{2free} = 15 s^{-1} and R_{2bound} = 150 s^{-1} as a function of bound fraction p_B, plotted for different dissociation rate constants k_{off}. In the fast exchange regime, R_{2av} interpolates linearly between R_{2free} and R_{2bound} as expected (Eq. 3). For slower exchange rates, R_{2bound} contributes less to R_{2av}. This effect is small for k_{off} = 1000 s^{-1} or greater, but becomes significant for k_{off} = 100 s^{-1} or less. For k_{off} = 500 s^{-1}, the initial slope at p_B = 0.1 deviates by about 10% from the limit of very fast exchange. Closely similar results are obtained for a wide range of R_{2free} rates (14% for R_{2free} = 5 s^{-1}; 5% for R_{2free} = 25 s^{-1}), whereas correspondingly increased k_{off} rates are required to achieve appropriate averaging of R_2 in the case of increased R_{2bound} rates (data not shown).

k_{off} > 500 s^{-1} is fulfilled only for weakly binding proteins. Association rates k_{on} for protein–protein pairs range from about 10^3–10^9 M^{-1} s^{-1} (Gabdoulline and Wade 2002). For k_{on} = 10^6 M^{-1} s^{-1}, k_{off} becomes greater than 500 s^{-1} for $K_D = k_{off}/k_{on}$ > 500 μM. The fast exchange condition is fulfilled for concomitantly smaller K_D values if the association rates are faster. In most situations, no information about the actual association rate is available, requiring other criteria to assess the fast exchange situation.

The best indicator of fast exchange on the relaxation time scale is the observation of the complete ^{15}N-HSQC spectrum of protein A in the presence of an excess of protein B. This control experiment may not be practical, if protein B is not very soluble. In this case, independent verification of the fast exchange situation on the relaxation time scale can be obtained by analysis of the exchange regime on the chemical shift time scale. This can be assessed using residues located at the protein–protein interface which change their chemical shifts between the free and bound state. Fast exchange on the chemical shift time scale is evidenced by gradual changes in the chemical shifts of protein A observed upon titrating protein B with protein A. Denoting the shift in frequency of the exchange-averaged signal of protein A from its position in the free state as $\Delta\nu_A$, $\Delta\nu_A$ increases, as expected, with the population of the bound state (p_B) and with the frequency difference $\Delta\nu_{(free,bound)}$ of protein A in the free state and in the 1:1 complex. Yet, $\Delta\nu_A$ is a non-linear function of k_{off}, being larger for faster exchange rates (Fig. 2B, C). Assuming that $\Delta\nu_{(free,bound)}$ does not exceed 2,400 Hz (corresponding to 3 ppm in a ^{1}H NMR spectrum at 800 MHz), one can set a boundary on the minimum k_{off} rate required to affect a $\Delta\nu_A$ value for a certain population of the bound state p_B. Figure 2C shows that, with all other parameters unchanged, the observation of, e.g., $\Delta\nu_A$ = 10 Hz at p_B = 0.1 indicates k_{off} > 2,500 s^{-1}. Therefore, observation of small gradual changes in $\Delta\nu_A$ values for interfacial residues upon titration of protein B with protein A can be sufficient to indicate k_{off} > 500 s^{-1} and hence, that the assumption of fast exchange on the relaxation time scale is valid for residues that do not change in chemical shifts between the free and bound states.

In measuring transferred $R_2(^{15}N)$ relaxation rates, care must be taken to avoid chemical exchange contributions which may be present in the complex but not in the free protein. Yet, since exchange contributions depend on differences in chemical shifts between the exchanging states, exchange broadening would be a problem only for ^{15}N-spins located near the protein-protein interface while the

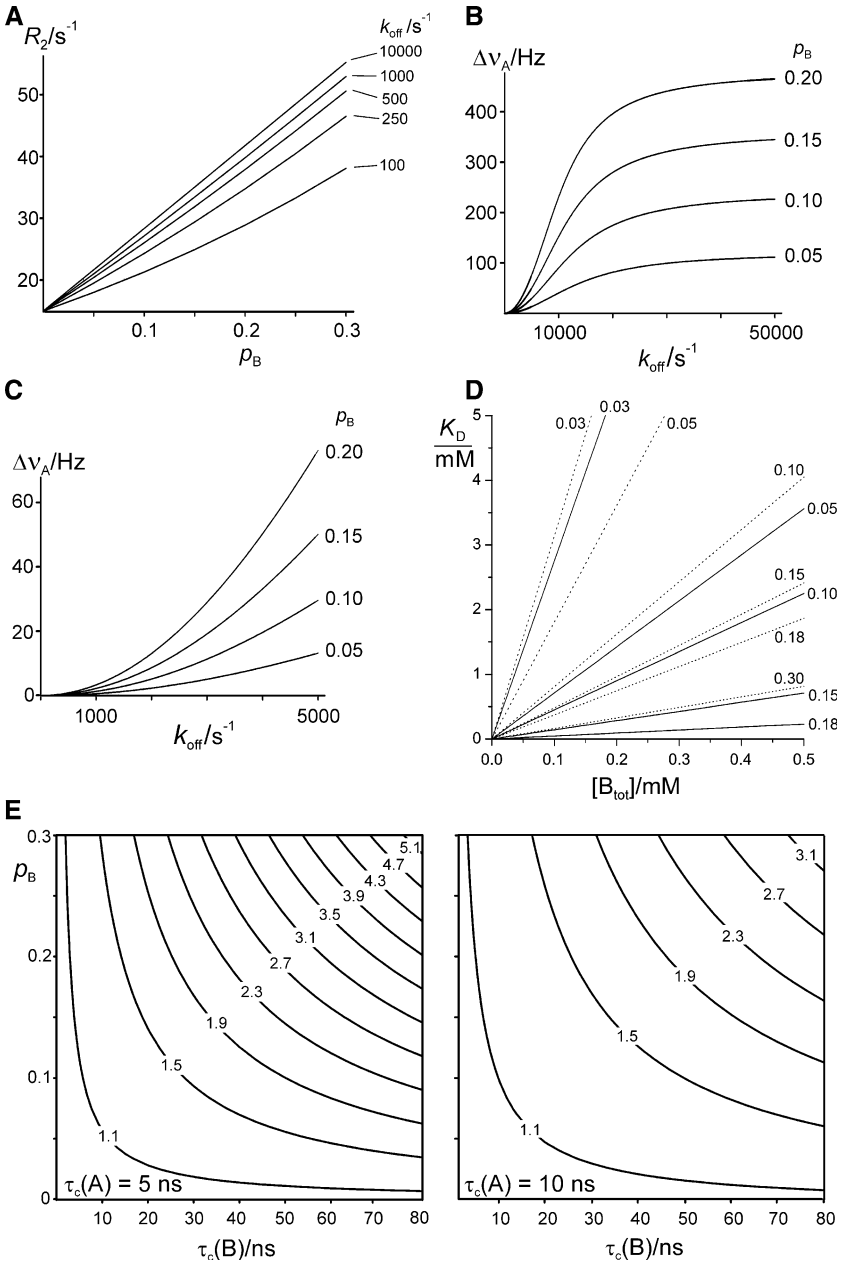

Fig. 2 Simulations for the design and evaluation of transferred relaxation experiments. Transferred $R_2(^{15}N)$-relaxation rates, chemical shifts and fraction of ^{15}N-labeled protein A bound to the unlabeled large protein B (p_B = [AB]/[A_{tot}]) were predicted for the equilibrium $[A] + [B] \rightleftharpoons [AB]$. (**A**) $R_2(^{15}N)$ relaxation rate *versus* the bound population p_B. The chemical shift difference between free and bound states was set to zero. R_2 values were obtained as $\nu_{1/2}\pi$, where $\nu_{1/2}$ is the full line width at half-height calculated using Bloch equations (Swift and Connick 1962; Sandström 1982). k_{off} is the dissociation rate constant of the complex. The curves were calculated for R_{2free} = 15 s^{-1} and R_{2bound} = 150 s^{-1} for the different k_{off} values indicated. The curve for k_{off} = 10000 s^{-1} is indistinguishable from a curve calculated using Eq. 3. (**B**) Frequency difference $\Delta\nu_A$ between protein A in the free state and in the presence of protein B plotted *versus* k_{off}. The curves were calculated assuming a frequency difference between the free and the bound states of 2400 Hz. They are labeled with the populations p_B used in the calculation. (**C**) Magnification of the curves in (**B**) for small k_{off} values. (**D**) Plot of the dissociation constant K_D *versus* the total concentration of the large protein [B_{tot}] for different populations p_B (indicated with each curve). Equation 4 was used with the ratios [A_{tot}]/[B_{tot}] = 1 (dashed lines) and 5 (solid lines). Use of a larger ratio [A_{tot}]/[B_{tot}] facilitates the measurement of $R_2(^{15}N)$ data (Fig. 3**B**–**D**), but limits the maximum achievable p_B value. (**E**) ^{15}N relaxation enhancement R_{2av}/R_{2free} as a function of the fraction of protein A in the bound state (p_B) and the rotational correlation time of protein B. The contour lines are labeled with the respective R_{2av}/R_{2free} ratios. The plots were calculated using the common equations of transverse ^{15}N dipole and chemical shift anisotropy relaxation of an isolated ^1H–^{15}N spin pair (Cavanagh et al. 1996), using a ^1H NMR frequency of 800 MHz. The rotational correlation time of the free protein A is indicated in the lower left corner of each panel. Readily measurable relaxation rate enhancements of over 50% are expected for a wide range of rotational correlation times and fractions of bound protein A (p_B)

chemical shifts of most remote ^{15}N-spins can be expected to remain unperturbed. Notably, a protein–protein complex which is in rapid equilibrium between bound and dissociated states tends to possess a small binding interface (Nooren and Thornton 2003). In this situation, most ^{15}N-spins can be assumed to report relaxation rate enhancements due to increased molecular weight without complications from exchange broadening. Their signals should conserve their chemical shifts in the complex and not display any excess line-broadening (Fig. 3A, B and E).

A final note concerns the assumption of a linear relationship between R_2 relaxation rates and molecular weight. This relationship is compromised in the case of non-spherical molecules, proteins with non-compact fold, and proteins composed of smaller domains which are linked by flexible polypeptide linkers. Accurate predictions of the average rotational correlation time can be made for proteins of known three-dimensional structure (Ryabov et al. 2006), but the shapes of the proteins studied may not always be known. Notably, however, the average rotational correlation time is not very much affected even by quite large deviations from a spherical shape. For example, using HYDRONMR (Garcia de la Torre et al. 2000), we simulated $R_2(^{15}N)$ relaxation rates for a spherical protein and for a protein with the same molecular weight but of an axially symmetric, elongated shape with an axial ratio of the diffusion tensor of 2.7:1. The average relaxation rate of the elongated protein was predicted to be only about 30% higher. Since the ^{15}N-relaxation rates depend on the orientation of the N-H bonds with respect to the diffusion

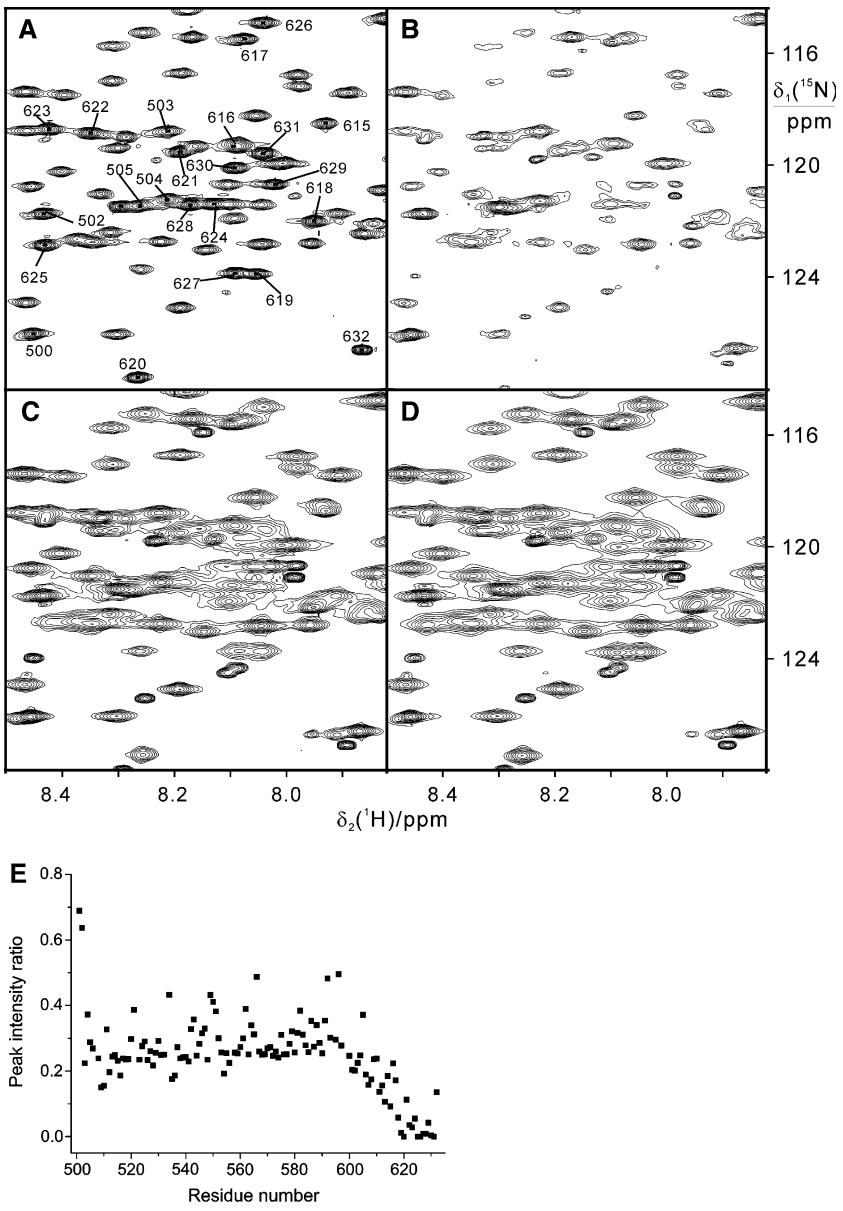

Fig. 3 Attenuation of the ^{15}N-HSQC cross-peaks of τ_C16Δ11 in the presence of α. Spectra were recorded of ^{15}N-labeled τ_C16Δ11 in the absence and presence of α at 25°C at a ^{1}H NMR frequency of 800 MHz. Only the central regions of the spectra are shown for improved visibility. (**A**) ^{15}N-HSQC spectrum of a 50 μM solution of τ_C16Δ11 in the absence of α. Cross-peaks of residues in the N- and C-terminal segments of the construct are identified with their sequence number. (**B**) 50 μM τ_C16Δ11 in the presence of 120 μM α. (**C**) 180 μM τ_C16Δ11 with 110 μM α. (**D**) 460 μM τ_C16Δ11 with 83 μM α. (**E**) Ratio of peak heights of τ_C16Δ11 in the absence and presence of 120 μM α, measured in the spectra shown in (**A**) and (**B**), respectively

tensor (Fushman et al. 2004), elongated proteins show much larger variation between the ^{15}N-relaxation rates of different amides, providing an indicator of non-spherical protein shapes. While a quantitative assessment of non-spherical shapes may be difficult, the error made by assumption of a single average rotational correlation time τ_C can be quite small (Fig. 1, Ryabov et al. 2006). Interestingly, estimating an average τ_C value from the molecular weight of calmodulin using Fig. 1 also yields a value close to the experimental value. This example shows that a flexible linker between two domains in a two-domain protein does not necessarily add great uncertainty to the estimate of R_{2bound} either.

Interaction between the C-terminal domain of the DNA polymerase III τ subunit and the α subunit

The use of transferred $R_2(^{15}N)$ relaxation rates for measurements of binding affinities was tested with the complex between the C-terminal domain of τ, a subunit of the *E. coli* DNA polymerase III complex, and the α subunit from the same enzyme complex. Whereas the C-terminal domain of τ binds with picomolar affinity to α (Gao and McHenry 2001) a domain shortened by 11 residues at the C-terminus ($\tau_C16\Delta11$) binds with an affinity that is too weak to be measurable in a BIAcore system or by gel filtration ($K_D > 10^{-5}$ M; Jergic et al. 2007). This raises the question: how much of the binding affinity is contributed by the C-terminal eleven residues of τ_C16 and how much by the rest of the protein? The molecular weights of $\tau_C16\Delta11$ and α are ~ 15,000 and ~ 130,000, respectively, and $\tau_C16\Delta11$ was uniformly ^{15}N labeled. Due to limited solubility of α (about 200 μM), it was used at a concentration of only 120 μM.

A ^{15}N-HSQC spectrum of a 50 μM solution of $\tau_C16\Delta11$ showed significant attenuation of the cross-peaks of the C-terminal residues (residues 618–631) in the presence of 120 μM α, with a few cross-peaks broadened beyond detection (Fig. 3A, B and E). In contrast, a control experiment using τ_C16 instead of $\tau_C16\Delta11$ failed to yield any ^{15}N-HSQC cross-peaks, indicating tight binding in a high-molecular weight complex with immobilization of the entire τ_C16 domain (data not shown). The selective line broadening observed for the C-terminal residues of $\tau_C16\Delta11$ thus indicates exchange broadening, in agreement with mutation data that localized the interaction site with α in the C-terminal 30 residues of τ_C16 (Jergic et al. 2007). The C-terminal residues of $\tau_C16\Delta11$ are also the only residues that change chemical shifts upon binding to α, except for a few residues in the N-terminal helix of $\tau_C16\Delta11$ which are spatially close to the C-terminal helix of the protein and therefore susceptible to indirect effects (Su et al. 2007). Exchange broadening is thus restricted to a relatively short segment of the protein. Further addition of $\tau_C16\Delta11$ resulted in shifts towards the peak positions of free $\tau_C16\Delta11$, indicating fast exchange on the chemical shift time scale. This suggested that the dissociation constant of the $\tau_C16\Delta11$–α complex could be measured by transferred ^{15}N-relaxation.

Measurements of R_{1free}, R_{2free}, R_{1av} and R_{2av} were made using a sample of free $\tau_C16\Delta11$ and a sample with $\tau_C16\Delta11$ in five-fold excess over α. In order to evaluate Eqs. 2 and 3, data were selected for residues in the structurally well-defined part of the protein which did not experience any chemical shift changes in the complex (Su et al. 2007).

The rotational correlation time of $\tau_C16\Delta11$ derived from the R_{2free}/R_{1free} ratio was 8.5 ns, as predicted for a monomeric 15 kDa protein. As expected for a small population of bound $\tau_C16\Delta11$, R_{1av} was very similar to R_{1free} (Fig. 4A and B). In contrast, R_{2av} was significantly larger than R_{2free} (28 s^{-1} compared with 18 s^{-1}; Fig. 4C and D). The molecular weight of the α–$\tau_C16\Delta11$ complex is about 145,000. Assuming a linear relationship between $R_2(^{15}N)$ values and molecular weight, R_{2bound} is therefore expected to be about 9.6*R_{2free}. This leads to p_B = 0.06 (Eq. 3). Therefore, only about 6% of $\tau_C16\Delta11$ were bound to α under the conditions of the experiment (total concentration of α = 83 μM; total concentration of $\tau_C16\Delta11$ = 460 μM). This corresponds to a dissociation constant K_D of 0.9 mM (Eq. 4).

Using the same parameters to calculate R_{1av} (Eq. 1), the R_{1av} and R_{1free} relaxation rates are expected to differ by only 6%. The experimental data (Fig. 4A and B) suggest an even smaller difference, which may be explained by limited experimental accuracy or residual mobility of $\tau_C16\Delta11$ in the complex.

The p_B value derived in this way allows verification of the fast exchange assumption. The largest chemical shift changes observed in the ^{15}N-HSQC spectrum were about 24 Hz measured in a sample of 90 μM $\tau_C16\Delta11$ and 110 μM α Under these conditions, K_D = 0.9 mM would have resulted in p_B = 0.10, *i.e.* the chemical shift change was sufficiently large to confirm that the exchange was fast on the relaxation time scale (Fig. 2C).

Combined with the subnanomolar affinity reported for the interaction of τ_C16 with α (Gao and McHenry 2001; Jergic et al. 2007), the present data show that the C-terminal 11 residues of τ_C16 contribute most (more than two thirds) of the binding affinity to α.

Concluding remarks

To design experimental conditions suitable for determination of a dissociation constant by transferred R_2 relaxation rate measurements, it is helpful to refer to plots of Eq. 4 (Fig. 2D) and relaxation rate predictions made for an

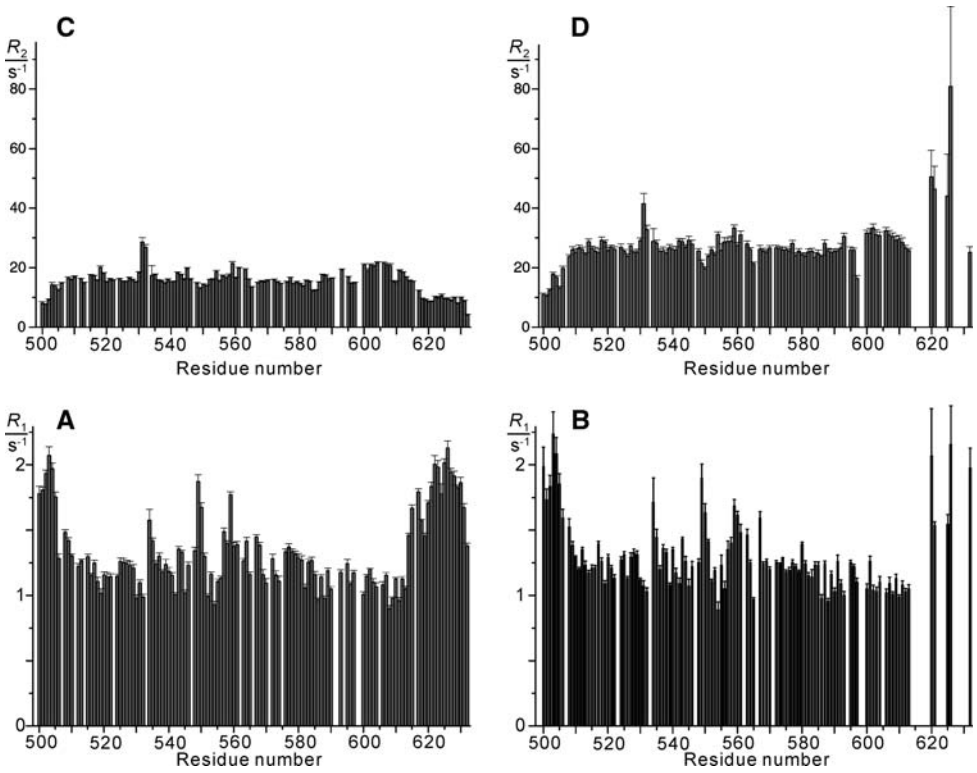

Fig. 4 ^{15}N-relaxation rates in ^{15}N-labeled τ_C16Δ11 in the presence and absence of α, measured at 25°C, pH 6.8. (**A**) Longitudinal relaxation rate R_1 of free τ_C16Δ11. (**B**) Longitudinal relaxation rate R_1 of τ_C16Δ11 in the presence of α. (**C**) Transverse relaxation rate R_2 of free τ_C16Δ11. (**D**) Transverse relaxation rate R_2 of τ_C16Δ11 in the presence of α. The largest changes were observed in the R_2 rates of residues following Leu619. The large uncertainties associated with the rate measurements of these residues in the presence of α were due to their broad line widths which prevented rate measurements for many of the residues beyond Gln613

isolated ^{15}N-^{1}H group (Fig. 2E). Fig. 2E shows that readily observable relaxation rate enhancements due to complex formation can be expected for a wide range of rotational correlation times of both proteins. If protein B has a high molecular weight, a p_B value as small as 0.03 may yield measurable relaxation rate enhancements. Figure 2D shows that $p_B = 0.03$ can readily be achieved even for K_D in the millimolar range, using small concentrations of the larger protein B. For a given concentration of protein B, the p_B value can also be tuned by the excess of protein A over protein B (Fig. 2D). In practice, the relative protein concentrations are best chosen in a titration experiment by inspection of the line-broadening observed in ^{15}N-HSQC spectra. The shortest measurement times are obtained for high concentrations of protein A, provided that significant and, hence, readily measurable line-broadening can still be observed, as in the spectra of Fig. 3A and 3D.

In conclusion, transferred R_2(^{15}N)-relaxation data offer a practical tool to measure the dissociation constant of a complex between a small ^{15}N-labeled protein and a large unlabeled protein, provided that the chemical exchange between bound and free protein is faster than the R_2-relaxation rate in the bound state. This condition is most readily fulfilled for dissociation constants in the high micromolar to millimolar range, but may also hold for more tightly binding protein–protein complexes if their dissociation rate is sufficiently fast. The fast exchange situation can independently be verified by checking for continuous chemical shift changes in a titration experiment.

For systems characterized by fast exchange, transferred relaxation measurements offer several attractive features: (i) they are suitable for high-molecular weight complexes, (ii) they do not depend on isotope labeling other than ^{15}N in the low-molecular weight protein, and (iii) the experiments can be performed with sub-millimolar protein concentrations. Although the accuracy of the K_D measurement is limited by the need to guess the relaxation rate of the complex, this estimate can usually be made with greater confidence than estimates of chemical shifts, translational diffusion constants, amide proton exchange rates or other parameters that could be measured by NMR spectroscopy. Therefore, K_D measurements by transferred relaxation present a useful addition to the toolbox of biomolecular NMR spectroscopy.

Acknowledgments This work was supported by the Australian Research Council, including project grants, a CSIRO-Linkage Fellowship (to K.O.) and a Federation Fellowship (to G.O.). S.J. held an International Postgraduate Research Award.

References

Barbato G, Ikura M, Kay LE, Pastor RW, Bax A (1992) Backbone dynamics of calmodulin studied by ^{15}N relaxation using inverse detected two-dimensional NMR spectroscopy: the central helix is flexible. Biochemistry 31:5269–5278

Bonvin AM, Boelens R, Kaption R (2005) NMR analysis of protein interactions. Curr Opin Chem Biol 9:501–508

Carlomagno T, Felli IC, Czech M, Fischer R, Sprinzl M, Griesinger C (1999) Transferred cross-correlated relaxation: application to the determination of sugar pucker in an aminoacylated tRNA-mimetic weakly bound to EF-Tu. J Am Chem Soc 121:1945–1948

Cavanagh J, Fairbrother WJ, Palmer AG, Skelton NJ (1996) Protein NMR Spectroscopy: Principles and Practice. Academic Press, San Diego

Clore GM, Gronenborn AM (1982) Theory and applications of the transferred nuclear overhauser effect to the study of the conformations of small ligands bound to proteins. J Magn Reson 48:402–417

Clore GM, Gronenborn AM (1983) Theory and applications of the transferred nuclear overhauser effect to the study of the conformations of small ligands bound to proteins. J Magn Reson 53:423–442

Dwek RA (1975) Nuclear Magnetic Resonance (NMR) in Biochemistry. Clarendon Press, Oxford

Farrow NA, Muhandiram R, Singer AU, Pascal SM, Kay CM, Gish G, Shoelson SE, Pawson T, Forman-Kay JD, Kay L (1994) Backbone dynamics of a free and phosphopeptide-complexed Src homology 2 domain studied by ^{15}N NMR relaxation. Biochemistry 33:5984–6003

Fushman D, Cahill D, Cowburn D (1997) The main-chain dynamics of the dynamin pleckstrin homology (PH) domain in solution: analysis of ^{15}N relaxation with monomer/dimer equilibration. J Mol Biol 266:173–194

Fushman D, Varadan R, Assfalg M, Walker O (2004) Determining domain orientation in macromolecules by using spin-relaxation and residual dipolar coupling measurements. Prog NMR Spectrosc 44:189–214

Gabdoulline RR, Wade RC (2002) Biomolecular diffusional association. Curr Opin Struct Biol 12:204–213

Gao D, McHenry CS (2001) τ binds and organizes *Escherichia coli* replication through distinct domains. Partial proteolysis of terminally tagged τ to determine candidate domains and to assign domain V as the α binding domain. J Biol Chem 276:4433–4440

Garcia de la Torre J, Huertas ML, Carrasco B (2000) HYDRONMR: prediction of NMR relaxation of globular proteins from atomic-level structures and hydrodynamic calculations. J Magn Reson 147:138–146

Garrett DS, Seok Y-J, Peterkofsky A, Clore GM, Gronenborn AM (1997) Identification by NMR of the binding surface for the histidine-containing phosphocarrier protein HPr on the N-terminal domain of enzyme I of the *Escherichia coli* phosphotransferase system. Biochemistry 36:4393–4398

Howard MJ, Chauhan HJ, Domingo GJ, Fuller C, Perham RN (2000) Protein-protein interaction revealed by NMR T_2 relaxation experiments: the lipoyl domain and E1 component of the pyruvate dehydrogenase multienzyme complex of *Bacillus stearothermophilus*. J Mol Biol 295:1023–1037

Jergic S, Ozawa K, Williams NK, Su X-C, Scott DD, Hamdan SM, Crowther JA, Otting G, Dixon NE (2007) The unstructured C-terminus of the τ subunit of *Escherichia coli* DNA polymerase III holoenzyme is the site of interaction with the α subunit. Nucleic Acids Res (in press)

John M, Pintacuda G, Park AY, Dixon NE, Otting G (2006) Structure determination of protein-ligand complexes by transferred paramagnetic shifts. J Am Chem Soc 128:12910–12916

Matsuo H, Walters KJ, Teruya K, Tanaka T, Gassner GT, Lippard SJ, Kyogoku Y, Wagner G (1999) Identification by NMR spectroscopy of residues at contact surfaces in large, slowly exchanging macromolecular complexes. J Am Chem Soc 121:9903–9904

Nakanishi T, Miyazawa M, Sakakura M, Terasawa H, Takahashi H, Shimada I (2002) Determination of the interface of a large protein complex by transferred cross-saturation measurements. J Mol Biol 318:245–249

Nooren IM, Thornton JM (2003) Diversity of protein-protein interactions. EMBO J 22:3486–3492

Otting G (1993) Experimental NMR techniques for studies of protein ligand interactions. Curr Opin Struct Biol 3:760–768

Peng JW, Moore J, Abdul-Manan N (2004) NMR experiments for lead generation in drug discovery. Prog NMR Spectrosc 44:225–256

Ryabov YE, Geraghty C, Varshney A, Fushman D (2006) An efficient computational method for predicting rotational diffusion tensors of globular proteins using an ellipsoid representation. J Am Chem Soc 128:15432–15444

Sandström J (1982) Dynamic NMR Spectroscopy. Academic Press, London

Su X-C, Jergic S, Keniry MA, Dixon NE, Otting G (2007) Solution structure of domain V of the τ subunit of *Escherichia coli* DNA polymerase III and interaction with the α subunit. Nucleic Acids Res (in press)

Sui X, Xu Y, Giovannelli JL, Ho NT, Ho C, Yang D (2005) Mapping protein-protein interfaces on the basis of proton density difference. Angew Chem Int Ed 44:5141–5144

Swift TJ, Connick RE (1962) NMR-relaxation mechanisms of O^{17} in aqueous solutions of paramagnetic cations and lifetime of water molecules in first coordination sphere. J Chem Phys 37:307–320

Takeuchi K, Wagner G (2006) NMR studies of protein interactions. Curr Opin Struct Biol 16:109–117

Vaynberg J, Qin J (2006) Weak protein-protein interactions as probed by NMR spectroscopy. Trends Biotechnol 24:22–27

Walters KJ, Gassner GT, Lippard SJ, Wagner G (1999) Structure of the soluble methane monooxygenase regulatory protein B. Proc Natl Acad Sci USA 96:7877–7882

Wijffels G, Dalrymple BP, Prosselkov P, Kongsuwan K, Epa VC, Lilley PE, Jergic S, Buchardt J, Brown SE, Alewood PF, Jennings PA, Dixon NE (2004) Inhibition of protein interactions with the β_2 sliding clamp of *Escherichia coli* DNA polymerase III by peptides from β_2-binding protein. Biochemistry 43:5661–5671

Zuiderweg ERP (2002) Mapping protein-protein interactions in solution by NMR spectroscopy. Biochemistry 41:1–7